Measurements of doping density in InAs by capacitance-voltage techniques with electrolyte barriers

D Frolov, G Yakovlev and V Zubkov

Department of micro- and nanoelectronics, St. Petersburg Electrotechnical University "LETI", Prof. Popov str. 5, St. Petersburg 197376, Russia

E-mail: frolovds@gmail.com

Abstract. The doping densities in n-InAs structures were studied by means of capacitance-voltage technique using electrolyte to form Schottky-like contact. It was shown that in heavily doped InAs ($> 10^{18}$ cm^{-3}) the depletion approximation can be used to obtain the true doping concentration. Concentration in low doped InAs can be estimated by simulation (using modified Thomas-Fermi approximation). Measured doping densities were compared with concentration obtained by Hall measurements. The difference between CV and Hall results in undoped samples was explained.

1. Introduction

Capacitance-voltage (CV) methods are widely used for characterization of semiconductor materials and structures [1–3]. Conventional CV measurements are performed by forming metal Schottky contact on semiconductor surface. However, in some semiconductor materials like InAs and InN the formation of reliable Schottky contact is difficult due to carrier accumulation at the surface, in this case an electrolyte can be used to form rectifying contact [4, 5]. Another advantage of electrolyte barriers, used in electrochemical capacitance-voltage (ECV) profiling technique, is the ability to perform controlled dissolution of the semiconductor [6, 7].

The interval of applied biases, in which depletion capacitance dominates, is very important for determination of doping densities by CV method with electrolyte barrier. In wide bandgap materials ($E_g > 2$ eV) this interval usually spans over more than 1 V and can be much higher for many semiconductors like Si, SiC, GaAs and GaSb at lower doping levels (approaching up to more than 6 V) [8].

The InAs, as a narrow band gap material, is very different in this regard. Gopal et al. [9] have reported on the ECV profiling of n-InAs. They noted that measured carrier concentration in highly doped InAs corresponds well to Hall measurements. For undoped InAs epi-layers it was noted that the measured CV concentration was much higher in comparison to Hall concentration, but no explanation was given.

The purpose of the present work is to explain the mismatch between CV and Hall results in undoped InAs samples and to determine the optimal parameters of CV measurements for doping density extraction in n-InAs.

2. Experimental and Simulation technique

Undoped InAs epi layers were grown by HVPE on n^+-InAs substrates. Doping densities were studied in undoped layers and in substrates. Capacitance-voltage measurements were performed using ECVPro profiler (Nanometrics). LCR meter Agilent E4980A was additionally connected directly to electrochemical cell to perform capacitance measurements in a wider frequency range. The aqueous solution of 0.2 M H_2SO_4 was used to form electrolyte barrier with nominal contact area of 0.1 cm^2.

CV characteristics were simulated by modelling potential and carrier distributions using Poisson equation with modified Thomas-Fermi approximation (MTFA) [10,11]. MTFA was used as an alternative approach to the self-consistent solution of Poisson and Schrödinger equations. To calculate capacitance the potential distribution must be found first. The potential as function of depth z must satisfy 1D-Poisson equation:

$$\frac{d^2\varphi(z)}{dz^2} = -\frac{q}{\varepsilon\varepsilon_0}\left[N_D^+ - N_A^- - n(z) + \ p(z)\right], \tag{1}$$

where ε is the dielectric constant of InAs, $n(z)$ and $p(z)$ are density of free electrons and holes. The donor (N_D) and acceptor (N_A) concentration were assumed constant throughout the space charge span range.

The distribution of electron density within MTFA was calculated as:

$$n(z) = \int_0^\infty \rho_c(z,E) f_{FD}(E) f_{MTFA}(z,E) dE, \tag{2}$$

where $f_{FD}(E)$ is the Fermi-Dirac function and $\rho_c(z,E)$ is density of state (DOS) function, which selected taking into account the conduction band nonparabolicity [12,13]:

$$\rho\,(z,E) = \frac{1}{2\pi^2}\left(\frac{2m_e^*}{\hbar^2}\right)^{3/2}\sqrt{E}\cdot\sqrt{1+\alpha E}\cdot(1+2\alpha E)\,. \tag{3}$$

Here $\alpha = (1 - m_e^*/m_0))^2/E_g$ is the nonparabolicity coefficient, and m_e^* is the effective mass of electrons.

The $f_{MTFA}(z,E)$ function in equation (2) is the MTFA correction function used to account boundary condition for the wave function at the semiconductor surface:

$$f_{MTFA}(z,E) = 1 - sinc\left(\frac{2z}{L}\left(\frac{E}{k_BT}\right)^{1/2}(1+\alpha E)^{1/2}\right), \tag{4}$$

where $L = \hbar/\left(2m_e^* k_B T\right)^{1/2}$ is the thermal length.

We numerically solved Poisson equation (1) using Dirichlet boundary conditions with $\varphi(\infty) = 0$. The capacitance per unit area was determined from charge increment over two applied voltages which differ by small step ΔV:

$$C = \frac{\Delta Q}{\Delta V} = \frac{\varepsilon\varepsilon_0 \Delta F_s}{\Delta V},$$

where $F_s = d\varphi(z)/dz|_{z=0}$ is the surface electric field.

3. Results and discussion

Experimental and simulated capacitance-voltage curves are shown in figure 1. All voltages in electrochemical cell were applied with respect to the reference Pt electrode. The main feature of the measured characteristics in comparison to ones for the many other materials (e.g. GaAs in figure 2c) is a strong deviation of C^{-2} vs. V plot from linear, which behave very similar

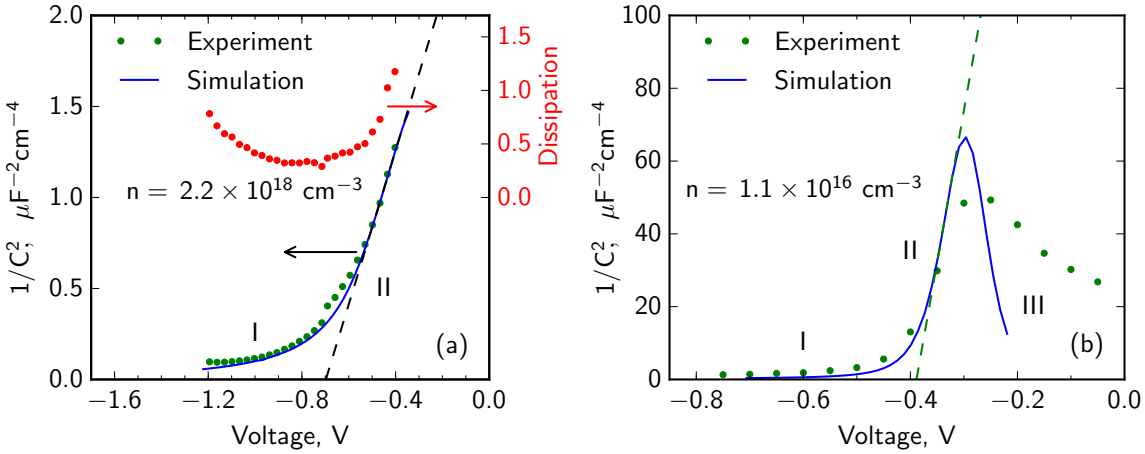

Figure 1: Mott-Schottky plot of experimental data and simulation for: (a) n-InAs substrate with $N_D = 2 \times 10^{18}$ cm^{-3} and (b) unintentionally doped InAs epi-layer ($n = 1 \times 10^{15}$ cm^{-3}). The electron densities calculated from linear fitting at the region II (dashed line) are also shown. The Roman numerals depicts: I – accumulation, II – depletion, III – inversion.

to CV characteristic of metal-oxide-semiconductor (MOS) structures. At lower biases, in the region of low positive slope of Mott-Schottky plot (region I in figure 1), the surface potential bends downwards which causes the formation of accumulation layer and increase of free carrier density. At higher positive voltages a depletion takes place. Here (region II) the slope of the Mott-Schottky plot is constant and proportional to the doping density. Further increase of bias leads to inversion which is characterized by a negative slope in C^{-2} vs. V curve (region III in 1b). The width in Volts of the transition region from depletion to inversion affects the accuracy of doping density measurements.

Another feature of InAs is its band position inside aqueous solution of electrolyte depicted in figure 2a. In this figure the band edge position of InAs is determined experimentally from Mott-Schottky plot as the difference between open circuit potential and flat-band potential

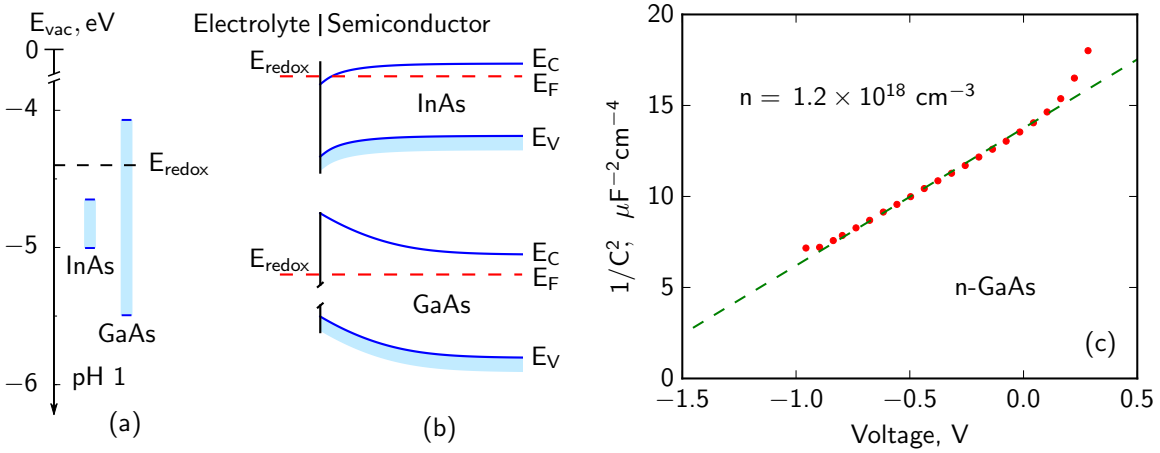

Figure 2: (a) Position of energy bands at the surface of InAs and GaAs in aqueous solution; (b) band diagrams of n-InAs and n-GaAs in equilibrium; (c) Mott-Schottky plot for n-GaAs.

relative to redox potential of electrolyte, the GaAs band edge position is given elsewhere [8]. It can be noted that in InAs the bottom of conduction band is located below the electrochemical potential (E_{redox}) of electrolyte which causes formation of accumulation layer in equilibrium (for $N_D < 10^{18}$ cm^{-3}), whereas in GaAs depletion arises (figure 2b) at any concentration.

Doping densities used in the simulation were obtained from magnetoresistance (for epi structure) and Hall effect measurements (for substrate) performed at 77 K. For n$^+$-InAs substrate the measured CV has a good agreement with simulation results (figure 1a). The dopant concentration of 2×10^{18} cm^{-3} was used for heavily doped n-InAs in simulation. Extraction of doping densities is usually carried out in voltage range, where dissipation factor is minimal. In our case it will give overestimated value of electron density (see figure 1a). To make accurate extraction of doping densities the voltage region, corresponded to depletion, should be used. The electron concentration calculated from linear approximation of C^{-2} vs. V curve in the depletion region gives 2.2×10^{18} cm^{-3}.

The difference between the dopant concentration used in the simulation and the calculated electron density is due to the small bias range of the depletion region. This difference is much higher for epi-layer with doping level of 1×10^{15} cm^{-3} (figure 1b) because the Fermi level shifts toward the center of forbidden energy gap, and the inversion starts earlier.

4. Conclusions

The measurements and simulations have shown that in heavily doped n-InAs ($n > 10^{18}$ cm^{-3}) the range of biases, in which the depletion occurs, is wide enough to use the depletion approximation for accurate doping density estimation. At the lower doping levels standard analysis of Mott-Schottky plot does not give the correct value of dopant concentration. In this case simulation of capacitance-voltage characteristics should be used to estimate doping density. The main reason of the mismatch between the true doping concentration and the concentration observed in CV measurement is the small band gap of InAs, leading to premature start of inversion. In general, to get accurate doping concentration in n-InAs one should choose the CV parameters, which results in formation of depletion region in wider voltage span range.

Acknowledgments

The investigation were carried out at Resource Center for Solid State Physics of SPbETU. In addition, authors would like to thank Dr. A.S. Petrov for fruitful discussion.

References

[1] Barnes P 2002 Capacitance–Voltage (C-V) Characterization Of Semiconductors *Characterization of Materials* (John Wiley & Sons, Inc.) pp 579–589
[2] Kucherova O V, Zubkov V I, Tsvelev E O, Yakovlev I N and Solomonov A V 2011 *Inorg. Mater.* **47** 1574–1578
[3] Hurni C A, Kroemer H, Mishra U K and Speck J S 2012 *J. Appl. Phys.* **112** 083704
[4] Yim J W L, Jones R E, Yu K M, Ager J W, Walukiewicz W, Schaff W J and Wu J 2007 *Phys. Rev. B* **76** 41303
[5] Vasheghani Farahani S K, Veal T D, Mudd J J, Scanlon D O, Watson G W, Bierwagen O, White M E, Speck J S and McConville C F 2014 *Phys. Rev. B* **90** 155413
[6] Blood P 1986 *Semicond. Sci. Technol.* **1** 7–27
[7] Zubkov V, Kucherova O, Frolov D and Zubkova A 2013 *Phys. Status Solidi C* **10** 342–345
[8] Memming R 2001 *Semiconductor electrochemistry* (John Wiley & Sons)
[9] Gopal V, Chen E H, Kvam E P and Woodall J M 2000 *J. Electron. Mater.* **29** 1333–1339
[10] Veal T D, Piper L F J, Schaff W J and McConville C F 2006 *J. Cryst. Growth* **288** 268–272
[11] Paasch G and Übensee H 1982 *Phys. Status Solidi B* **113** 165–178
[12] Ariel-Altschul V, Finkman E and Bahir G 1992 *IEEE Trans. Electron Devices* **39** 1312–1316
[13] Bebb H B 1971 *J. Appl. Phys.* **42** 3189–3194